Research and Design of Belt Deviation Detection System Based on Single-side Rollers

Peng Zhang, Shaochuan Xu and Minghao Ma

Abstract—**Belt conveyors often work in more complex environments, although many are indoors. However, due to the structure of the plant and other reasons, it is difficult to install the camera directly above the belt when using the camera to monitor the belt or identify faults. At this time, the staff can only find a location as far as possible can play a role in monitoring the belt conveyor to install the camera. In this case it is more difficult to analyze whether the belt is running away. On the other hand, the previous belt deflection detection method is through the artificial delineation of the standard position of the belt, the actual position of the belt and the standard position for comparison, which to a large extent there are human factors interference, resulting in the detection results are not precise enough. Therefore, in this paper, for the belt that can only monitor the type of unilateral rollers, we propose a method to recognize whether the belt is empty or not, and then determine the standard position of the belt through a multi-task learning model with joint target detection and semantic segmentation. This enables adaptive recognition of the standard position of the belt. The degree and direction of belt deflection is determined by obtaining the line connecting the straight line at the edge of the belt and the uppermost corner point of the rollers. The overall accuracy of the system is 94.9%, which is obtained by experimenting with the multi-task learning model and the belt runout judgment model respectively. It can be concluded that the belt runout detection method proposed in this paper can be a good solution to the situation where the camera installation position is not ideal. It reduces the failure rate of the belt conveyor and provides a guarantee for the normal operation of the belt conveyor.**

Index Terms—**belt conveyor, belt deviation, belt unloading, multi-tasking learning**

I. INTRODUCTION

Belt conveyors as the main conveying equipment in coal and other industries [1]. In general, when transporting materials, multiple belts are used for coordinated transport. It is a practical and continuous type of transportation. In coal transportation, it plays an irreplaceable role. In actual production, belt conveyors are characterized by large transport capacity, long transport distance and space saving. However, belt deviation is a kind of failure that occurs more frequently and can cause some other failures when the deviation is serious [2]. At present, many experts and scholars have studied the belt deviation phenomenon and proposed many methods for belt deviation detection. In order to be able to solve the frequency of belt deviation failure as much as possible. For example: Wang, Xu, and Teng proposed a method to enhance the features of belt edges through the operations of image expansion, erosion, and binarization processing, and then identify the edge position of the belt through the method of Hough linear detection, so as to determine whether belt deviation faults occur [3]. Wang et al. combining an Internet of Things (LoT) platform and a Lightweight Gradient Lifter (LGBM) model to build a belt conveyor fault diagnosis system. Collecting data during belt operation by installing sensors, and finally building LGBM models to diagnose belt conveyor faults. Its evaluation index and K-fold cross-validation prove the validity of the model [4]. A deep learning based belt deviation detection method was proposed by Zhang et al. By improving the YOLOv5 model for belt deviation detection, the problem of fast feature extraction and deviation detection of belt edges in complex backgrounds is effectively solved [5]. Yu et al. defined the taper correlation index by the outer cylindrical surface of the rollers and designed a method for automatic detection of belt deviation, and established an error processing model for the data according to the actual conditions of detection and the working mechanism of the relevant sensors [6]. Chen et al. proposed a real-time belt detection method based on multi-scale feature fusion network. The performance of the detection network is improved by fusing the underlying features with rich location and detail information with the higher-level features with stronger semantic information through a multi-scale feature fusion network, and a new weighted loss function is designed to improve the detection of belt edges [7].

The currently proposed belt deviation detection method can achieve good results in the face of some routine situations. However, this does not apply to the case mentioned in this paper where only one side of the rollers and the edge of the belt can be monitored. Therefore, this paper proposes a belt deviation detection method for the case of unsatisfactory camera installation position. The contributions of this paper are: Firstly, we propose a method to define the standard belt position by determining whether the belt is empty or not. Next, the belt and rollers are divided by a multi-task learning model, and a belt deviation judgment model is established to calculate the degree and direction of belt deviation. The accuracy of the method is proved to be high through

experiments in the field, and it can meet the actual requirements of the belt conveyor work site.

II. SINGLE-SIDE ROLLER WORKING CONDITION TYPE ANALYSIS

For single-side rollers, it is mainly caused by the installation position of the camera. The structure of the plant in which this type of belt conveyor is located does not lend itself to the installation of a camera device in a normal location, and it is only possible to find a location where the belt conveyor can be monitored. The ideal placement of the camera is shown in Fig. 1. The camera for image acquisition in Fig. 1 is mounted directly above the belt. There is a certain distance between the lighting and the camera, the environment plays a good lighting effect, and will not be too close to the camera to cause the camera backlight. The camera installed in this location captures the complete information about the characteristics of the belt conveyor, both during the day and at night, and the belt deviation can be determined by using basic straight line detection or edge detection.

Fig. 1. Diagram of the ideal installation position of the camera

(a) Daytime images

(b) Night image

Fig. 2. Types of working conditions of single-side rollers

However, the camera position shown in Fig. 2 is diagonally above the belt conveyor. Due to factors such as plant structure it is not possible to mount the camera at the angle shown in Fig. 1. Acquisition of images from this angle makes it difficult to determine the relative position between the rollers and the belt near the camera side. If deviation detection is performed for this type of belt, it can only be judged by the side away from the camera, and from Fig. 2, the color characteristics of the guardrails on both sides of the belt conveyor are similar to the color characteristics of the belt, which can easily cause interference to the detection system [8].

The application of NI VISION or some other traditional machine vision tools can achieve the detection of single-sided belt deviation in some conditions where the relative position of the camera is good. But careful observation of the image can be found, away from the camera side of the belt near the edge of the existence of some metal guardrail, and the edge of the belt closer distance. In order to protect the personal safety of the staff on site, and can not remove the guardrail. With such a sampling angle, the detection area of the whole image can be divided into two regions A and B. As shown in Fig. 3, if the ROI is delineated on the side away from the camera using algorithms such as straight line detection or edge detection to extract the belt edges. Since the A area is far away from the camera position, the area occupied by the rollers in the image is small, and some feature information on it is weakened accordingly [9]. So it is not suitable as a detection area, and the guardrail in area A will also be revealed when the belt runs to the other side, which will easily affect the detection; Area B is closer to the camera and the features of the rollers and belt are obvious though. But due to the angle, the guardrail almost overlaps with the edge of the belt. This leads to a higher chance of algorithm misclassification, which can easily misclassify the guardrail as a belt edge.
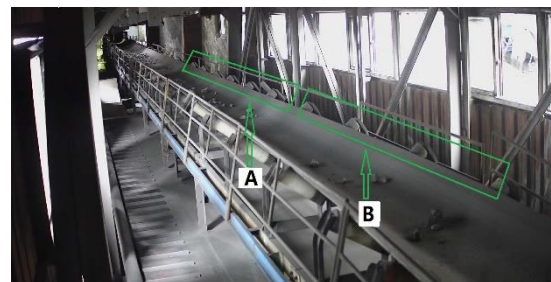
Fig. 3. Detection area division

The effect of the guardrail influence when extracting the belt edge using straight line detection is shown in Fig. 4. The upper edge of the guardrail is detected directly as the edge of the belt in Fig. 4. The ability to detect the edge of the belt when it runs diagonally upwards in the image and covers the guardrail; However, when the belt runs diagonally downward in the image, it is easy to misjudge the guardrail as the edge of the belt. This will directly cause the input data of the subsequent judgment system to remain constant, making the entire belt deviation detection system ineffective.
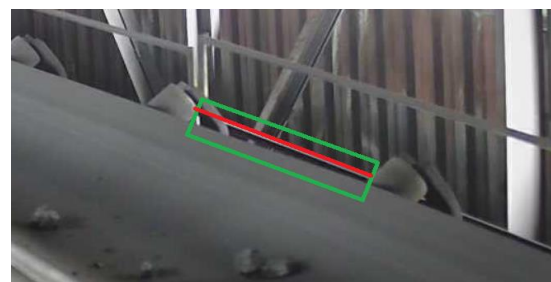
Fig. 4. The effect of being affected by the guardrail

If the width of the ROI area is reduced so that it is below the guardrail, the edge of the belt can be accurately identified, as shown in Fig. 5. However, the width of the ROI area is reduced, which in turn leads to a reduction in the detectable area. A small deviation of the belt during operation can cause the edge of the belt to fall out of the ROI detection range, making it impossible to determine the direction and magnitude of the deviation; On the other hand, the belt conveyor will continue to sway slightly from side to side during operation. If the width of the ROI area is reduced, the belt edge will easily trigger the deviation detection threshold. This leads to frequent alarms in the alarm module of the detection system, at which point the belt deviation detection system as a whole becomes meaningless.
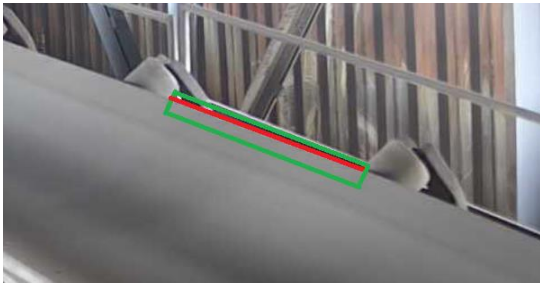
Fig. 5. Narrowing the ROI detection area
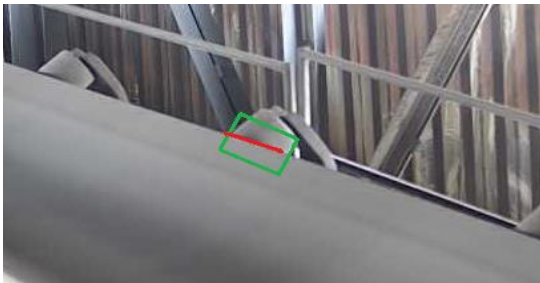
Fig. 6. Replace ROI area

Looking at the whole image, only the edge of the belt above the rollers in area B is not affected by the guardrail, as shown in Fig. 6. However, the relative area of the rollers in the graph is small and the area of the ROI region is affected by the area of the rollers. Due to the location of the camera relatively far from the belt conveyor. Once there is a small shift in the camera position, the relative position of the ROI area changes drastically and the probability of misclassification increases.

III. DETECTION METHOD SELECTION

Based on the above analysis of the type of single-side rollers, we can learn that traditional methods such as linear detection or edge detection are not able to play a good detection effect. To a certain extent, it will be affected, resulting in the loss of effectiveness of the detection system. On the other hand, most of the current belt deviation detection methods require manual setting of the standard belt position. This will be subject to human interference, resulting in some deviation in the calculation of the degree of belt deviation. Therefore, this paper proposes a multi-task learning approach based on joint object detection and semantic segmentation to achieve belt deviation detection.

A. Multi-task learning model

The model is a simple feed-forward network, but it is efficient in its execution, allowing simultaneous detection and segmentation of the belt, rollers and material. As shown in Fig. 7, the model is an encoder-decoder architecture containing a multitasking shared encoder and two decoders used to implement specific functions. There are no other complex shared units between decoders to reduce the parameters of the network and increase the training efficiency of the model [10].

The network shares an encoder structure, for which the encoder part of the model is mainly composed of Backbone and Neck parts. The Backbone section is mainly used to extract the features of the image. Generally speaking, the feature extraction networks of the more classical image classification networks are able to be used as encoders. Based on YOLOv5's excellent feature extraction performance. Therefore, in this paper, the feature extraction network of YOLOv5_v6.0 is selected as the encoder, which mainly includes CBS and C3. The CBS layer is composed of Conv+BN+SiLu activation functions. YOLOv5 uses C3 structure instead of the original BottleneckCSP structure. Reducing the model parameters while also improving the learning ability of the model saves a lot of computational resources [11].

In the Neck section, SPPF is used in combination with FPN to obtain better feature fusion. For SPPF structures, which specify a convolution kernel. The output of each pooling becomes the input of the next pooling, and the response speed is faster compared to SPP. The use of SPPF structure also improves the ability of the model to handle different scale targets, obtain contextual information and adapt to different input sizes, which helps to improve the accuracy and robustness of the algorithm [12]. FPN is often used in semantic segmentation tasks. By combining with encoders, the network can simultaneously obtain multi-scale feature representations and rich semantic information. The FPN module obtains feature pyramids with richer semantic information through feature fusion, and FPN can also provide a pyramid feature fusion mechanism. Feature fusion and pooling operations are performed by different layers in the pyramid to generate fixed-size feature representations, thus providing more comprehensive contextual information for target detection and semantic segmentation [13]. Therefore, combining the two can make better use of multi-scale features and contextual information to improve the performance of the model in the face of complex scenarios.

The detection head and segmentation head in this network model are decoders for two different tasks. Use PAN structure in the detection head part, PAN is a bottom-up feature pyramid network [14]. The PAN module is capable of cascading high-resolution features with low-resolution features. Generally speaking, low-resolution features have a wider field of view and richer contextual information, while high-resolution features contain more detailed information. PAN is able to capture multi-scale semantic information while retaining detailed information. Dynamic adaptation according to the scale of the ingested feature map enables the model to better handle targets of different scales [15].

In the segmentation head section. The bottom feature layer of the FPN is used as the segmentation head with the size of

(W/8,H/8,256). The segmentation part of the model is relatively simple. After three up-sampling, the output feature map size is recovered to (W,H,256). Since the SPPF structure is already used in the Neck part, it is not added in the segmentation head part, thus ensuring the real-time inference process [16].

In this network model there are two decoders, each with its own unique loss function. In terms of the detection loss function, the overall loss L_{det} of the detection part is the weighted sum of the classification loss, localization loss and confidence loss. The expression is shown in Equation 1.

$$L_{det} = \alpha_1 L_{cls} + \alpha_2 L_{box} + \alpha_3 L_{obj} \qquad (1)$$

Where L_{cls} is the classification loss, which is mainly used to calculate whether the anchor frame is correctly classified with the corresponding calibration. L_{box} is the localization loss, which uses the GIoU to reflect the error between the prediction box and the calibration box. L_{obj} is the confidence loss, which is used to calculate the confidence level of the network [17].

For the segmentation loss function, the cross-entropy loss function L_{ce} is used. The expression is shown in Equation 2.

$$L_{seg} = L_{ce} \qquad (2)$$

Therefore, the final loss function of this model is the weighted sum of the detection loss and the segmentation loss. As shown in equation 3.

$$L_{det+seg} = \beta_1 L_{det} + \beta_2 L_{seg} \qquad (3)$$

In which the importance of each part of the loss can be weighed according to the size of α_1, α_2, α_3, β_1, β_2, so that the overall loss is balanced.

B. Belt deviation detection method

According to the analysis of the actual situation on site, from the belt operation law and the cause of runaway. The probability of belt deviation at no load is negligible. Almost all belts can be automatically adjusted to the standard position at no load. To verify that the belt can automatically adjust to the standard condition at no load. In this paper, a number of belts with single side rollers are selected. After the belt has been running empty for a period of time, the belt conveyor is stopped in order to ensure the safety of the staff on site. The relationship between belt position and belt idle load is verified by manual measurement. By measuring the actual position of multiple belts at no load and the relative position between the rollers on both sides. From the measurement results, it can be concluded that all belts are able to adjust themselves to the standard position after the belt is running at no load. Although there is a small error, it will not affect the belt deviation detection. Therefore, this paper defines the standard position of the belt by judging whether the belt is empty or not for the working condition of single-side rollers. The actual position of the belt during operation is then compared with the standard position to determine the degree and direction of belt deviation [18].

C. Model training and detection results

According to the above proposed method of defining the standard position of the belt. Need to identify and segment the belt, the rollers and the material transported on the belt by multi-task learning. The encoder part of the model uses the feature extraction network of YOLOv5. Therefore, the training process is relatively simple, just put the data into the model with good labeling and training. The model was trained for 200 epochs and the model was able to converge well. The accuracy rate of identifying and segmenting the rollers is 93%, the accuracy rate of identifying and segmenting the belts is 95.1%, and the accuracy rate of identifying and segmenting the materials is 91.6%. The specific data are shown in TABLE I.

TABLE I
MULTI-TASK LEARNING MODEL EVALUATION INDEX DATA

classes	P	R	AP
belt	0.951	0.943	0.949
roller	0.930	0.917	0.919
coal	0.916	0.921	0.920
all	0.932	0.927	0.929

The detection effect of multi-task learning is shown in Fig. 8. As can be seen from the inspection results, the model has a complete and high definition of the edges of the belt, rollers and material division. Regionalization of the categories to be recognized by a semantic segmentation task. Naming the categories to be detected by the object detection task. In this way, it provides a reliable guarantee for the determination of the amount of coal transported on the belt.
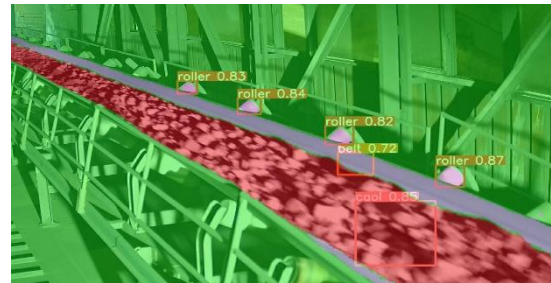
Fig. 8. Multi-task learning detection effect

IV. BELT DEVIATION DETECTION BASED ON SINGLE-SIDE ROLLERS

A. Defining the standard position of the belt

For the single-side roller type of work, due to the installation position of the camera can not completely capture the overall belt conveyor. In order to ensure that its definition of the standard position can be more accurate and avoid deviations when defined manually. Therefore, this paper uses the standard position of the belt by detecting whether the belt is empty or not for belt conveyors in this situation.

Belt no-load judgment is also to detect whether there is material being transported on the belt during the operation of the belt. Belt conveyors are mostly used to transport coal. Therefore, in order to determine whether the belt is empty, it is only necessary to check whether there is coal on the belt. The multi-task learning model selected in this paper can achieve both object detection and semantic segmentation. As shown in Fig. 9, the distribution of material on the belt is continuous and shows an irregular shape. Integrated judgment combining two tasks of object detection and

semantic segmentation. When the result of the two tasks is the presence of material, the belt is in the material state. When the detection result of both tasks is that no material is present, the belt is empty. As shown in Fig. 10, when the belt is empty, the model only detects the "belt" and "roller" categories. The model can detect all three categories of "belt", "roller" and "coal" when there is material on the belt. Therefore, it can be determined whether the belt is at no load or not.

Fig. 9. Material distribution
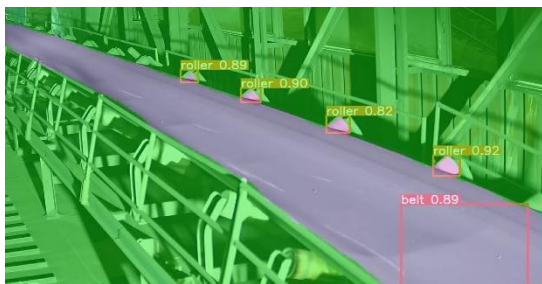
(a) Belt no-load condition
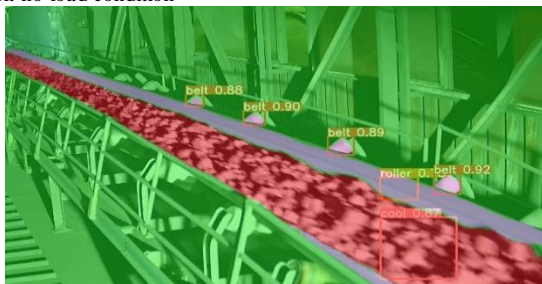
(b) Belt with material status
Fig. 10. Belt material detection

B. Coordinate system conversion

The belt is a gradual process from material to no load. During the actual transportation process the material will gradually decrease and eventually reach the empty state. During this process the load on the belt decreases and the belt will adjust itself to the standard position. When the belt is completely unloaded, the belt can be adjusted to the standard position. Take screenshots of the belt work video at regular intervals. The belt will also shake slightly around the standard position when running at no load. When the first fully unloaded image is detected, the position of the belt in this image is obtained, and the coordinates of the pixel points at the edge of the belt and the topmost corner of the rollers are extracted. But in the image is the upper leftmost point of the image as the origin, horizontal to the right as the x-axis, vertical down as the y-axis. Using the original coordinates can be troublesome for calculating deviation values. Therefore, the coordinate system needs to be converted. Convert the image coordinate system into a mathematical

coordinate system, with the center of the image as the origin, the x-axis horizontally to the right and the y-axis vertically up. It can not only improve the accuracy of the detection system, but also ensure the maximum real-time detection system.

The image is composed of a large number of pixel points, and the image is represented as an M*N matrix of pixels. For the upper leftmost point in the image, the coordinates in the image coordinate system are (0,0) and in the mathematical coordinate system are (-N/2,M/2). Then the conversion relation of a pixel point (x',y') in the image to the mathematical coordinate system (x,y) is shown in Equation 4, where x is the column and y is the row.

$$\begin{cases} x = x^{'} - \dfrac{N}{2} \\ y = -y^{'} + \dfrac{M}{2} \end{cases} \qquad (4)$$

C. Least squares fitting

Pixel dots at the edge of the belt show a stepped distribution. However, the edges of the belt show an irregular stepped shape due to wear at the edges. After extracting the belt edge pixel points and the topmost corner points of the carrier rollers. Converting the pixel coordinates in the above manner results in a new set of coordinates. If the equation of the line is found by taking two points directly at the edge of the belt in the same way as two points determine a line, will result in a large error between the slope of the found line and the actual slope. So two points cannot be used to determine the straight line of the belt edge.

In this paper, the least squares method is chosen to fit the coordinates of the pixel points at the edge of the belt. Least squares is an optimization method that minimizes the sum of squares of errors as a way to determine the best fit function for unknown data. The method is mainly used in the field of data prediction, curve fitting, etc. The mathematical expression is shown in Equation 5.

$$E_i(p) = \sum_{i=1}^{m}\left[f_i(p) - \varphi_i(p)\right]^2 = \min\sum_{i=1}^{m}\left(F_i(p) - \varphi_i(p)\right)^2$$
$$F_i(p) \in F_m(p) \qquad (5)$$

Due to the large number of extracted pixel points, the interference points present in them are not easy to find. So all the sample points are divided into groups according to a group of three points, and then one point from each group is taken as the sample point for the fit. In this paper, the edge of the belt away from the camera side, the uppermost corner point of the rollers are fitted. The straight line after the least squares fit is shown in Fig. 11.

In order to verify whether the outermost connection line of the same side of the rollers and the edge of the belt are parallel, the slope of the two straight lines on the same side are compared and there is only a slight error in the fractional part. The main reasons for the existence of errors are the following: (1) The belt conveyor has long overload operation, there is a slight deformation, resulting in deviations in the slope of the belt edge on the same side and the outermost connection line of the carrier roller; (2) Despite the already high accuracy of deep learning models, they can suffer in the complex working environment in the field; (3) Individual sample points can also introduce some errors when fitting

using least squares. According to the actual requirements of the site and the selection of the deviation judgment method, the slight error does not affect the system as a whole and is within a reasonable error range, so the error of the straight line slope on the same side is negligible.
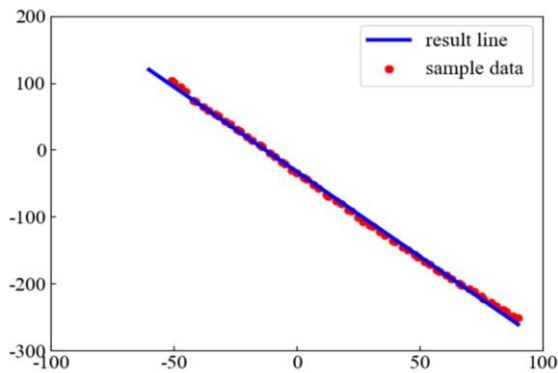
(a) Topmost corner connection line of rollers
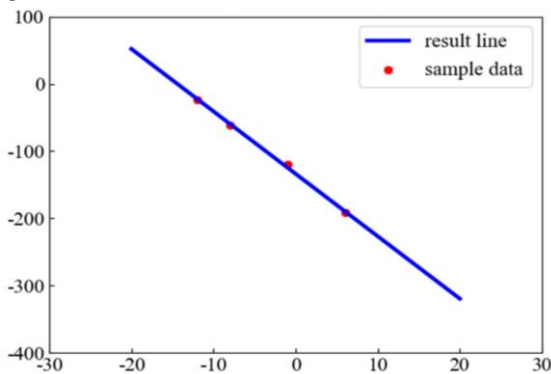
(b) Belt edge straight line

Fig. 11. Least Squares Fitting

D. Establishing a model for judging belt deviation with single-side rollers
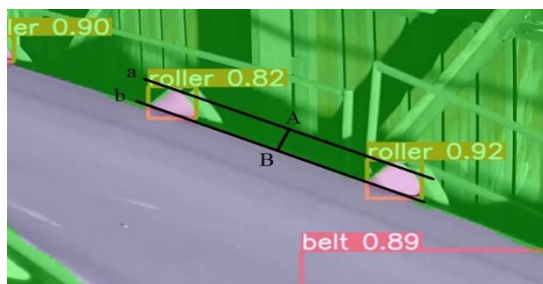
(a) Define standard location
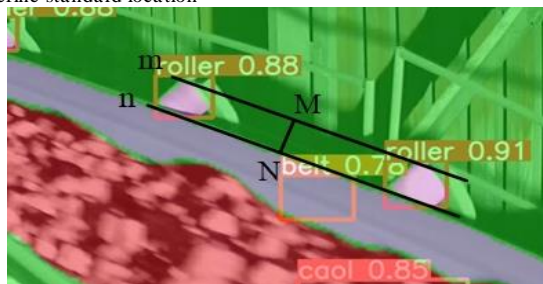
(b) Actual distance between belt and roller

Fig. 12. Judgment of belt deviation with single-side rollers

As shown in Fig. 12, when the belt is detected to be at no load, the standard position of the belt starts to be derived from the distance between the edge of the belt and the uppermost corner point of the roller. Straight line *a* and straight line *b* are

the lines fitted by least squares method respectively. Take the points $A(x_A, y_A)$ and $B(x_B, y_B)$ on the lines *a* and *b* respectively, and the line segment *AB* is perpendicular to the lines *a* and *b*. Then the length of the line *AB* when the belt is in the standard position is:

$$AB = \sqrt{(x_A - x_B)^2 + (y_A - y_B)^2} \tag{6}$$

When material is detected on the belt, it proves that the belt is running. The belt will move in the direction of material transportation, accompanied by the phenomenon of deviation. At this point, obtain the straight line *n* and the straight line *m* fitted to the edge of the belt and the uppermost corner point of the rollers. Take the points $N(x_N, y_N)$ and $M(x_M, y_M)$ on the line *n* and the line *m* respectively, and the line segment *MN* is perpendicular to the line *m* and the line *n*. Then the distance between the edge of the belt and the uppermost corner point of the roller when the belt is running is:

$$MN = \sqrt{(x_M - x_N)^2 + (y_M - y_N)^2} \tag{7}$$

Then the actual deviation distance d of the belt is:

$$d = |MN - AB| \tag{8}$$

The line *AB* is the distance between the edge of the belt and the uppermost corner of the rollers when the belt is in the standard position, so it is also the maximum deviation distance of the belt. Under normal circumstances, the lengths reserved by the rollers on the left and right sides of the belt are equal, so no matter which direction the belt deviates, the maximum deviation distance is the length of the line *AB*. So the deviation percentage of the belt is:

$$\mu = \frac{d}{AB} \times 100\% \tag{9}$$

The deviation direction of the belt can be determined by the size of the line *AB* and the line *MN*. When *AB>MN*, the belt deflects to the side near the camera; When *AB<MN*, the belt runs to the side away from the camera. From this, the degree and direction of belt deviation can be found.

V. Test results and system implementation

A. Deep learning model validation

Validation of the deep learning model by selecting 3000 test data. The test set images are all of the type where the camera can only monitor one side of the belt edge and the rollers. It contains 1000 images with good environmental conditions and 2000 images affected by light and dust. The trained model was tested, in which a total of 2,856 images were able to segment the belt, rollers and materials with accurate recognition rate, with an accuracy rate of 95.2%. The statistical table of the effect of the deep learning model is shown in TABLE II.

TABLE II
DEEP LEARNING MODEL EFFECT STATISTICS

Category	Better detection + segmentation	Poor detection + segmentation	Total
Light and dust	1892	108	2000
Better environmental	964	36	1000
Total	2856	144	3000
Percentage	95.2%	4.8%	100%

According to the data in TABLE II, it can be seen that the

images with better implementation of the target detection task and the semantic segmentation task in the type of working conditions of the unilateral rollers account for 95.2% of the corresponding test images. Analysis of images with poor results, the main reason is that individual belt sections have serious belt edge wear, and many burrs appear near the belt edge, resulting in a lot of interference points in the segmented effect picture. Another case is that the idle rollers in the background screen of individual images are also detected. In this case, just need to block the idle rollers in the background or move them out of the camera's field of view. But the identification of the belt and rollers by the belt edge wear is inevitable, and the wear of the belt interval section is small, the overall impact on the detection system will not be too big.

B. Belt deviation judgment model validation

To verify the belt deviation judgment method. Firstly, the belt deviation degree should be classified, and the specific belt deviation degree judgment criteria are shown in TABLE III.

TABLE III
JUDGMENT CRITERIA FOR BELT DEVIATION

Degree of deviation	Range of interval
Normal state	$0 \leq \mu < 20\%$
Mild deviation	$20\% \leq \mu < 50\%$
Heavy deviation	$\mu \geq 50\%$

The detection method of single-side rollers working condition is tested, and 2,856 images with better recognition effect of multi-task learning model are used to judge the degree of deviation. It contains 987 images of normal state, 1035 images of mild deviation state and 834 images of heavy deviation state. The judgment method was tested and the test results are shown in TABLE IV.

By analyzing the data in TABLE IV, the number of misjudgments of the test methods selected in this paper for the single-side rollers working condition is 8 respectively, and there is no phenomenon of missed detection. The number of final correct judgments was used to calculate the overall accuracy rate, and the final accuracy rate was 94.9%. Therefore, it can be concluded that the belt detection method proposed in this paper can still maintain a high accuracy rate in the case that the site environment is not ideal, which basically can meet the actual needs of the site and has some practical value.

VI. DESIGN AND IMPLEMENTATION OF BELT DEVIATION DETECTION SYSTEM BASED ON SINGLE-SIDE ROLLERS

A. System function module
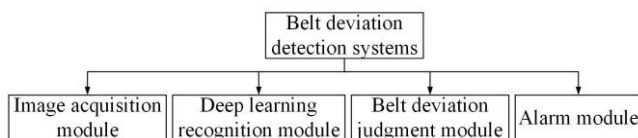
Fig. 13. System function module

The belt deviation detection system designed in this paper is divided into four modules, which are: image acquisition module, deep learning recognition module, belt deviation judgment module and alarm module. The functional modules of the system are shown in Fig. 13.

The functions that each module can perform are as follows:

(1) Image acquisition module

The image acquisition module is mainly responsible for the acquisition and transmission of images or videos of the belt conveyor in operation. Acquisition of images on site by calling the SDK file of the Hikvision device. This is used to obtain experimental data and to be able to continue image acquisition after the system is put into use.

(2) Deep learning recognition module

The deep learning recognition module focuses on the recognition of belt conveyors. Segmentation and detection of belts, rollers and materials through combined object detection and semantic segmentation tasks. The main role of the deep learning recognition module is to identify and segment the target, providing good support for the subsequent belt deviation judgment module.

(3) Belt deviation judgment module

The belt deviation judgment module is mainly based on the deep learning recognition effect, and calculates the relative position of the belt and the rollers, so as to judge the degree and direction of belt deviation.

(4) Alarm module

The alarm module mainly issues an alarm to the field staff when the belt deviation reaches a certain threshold, prompting the staff to deal with the belt deviation in time. To avoid causing greater failure or even some safety hazards. The belt will shake from side to side during operation, and the percentage of belt deviation identified at each moment is different. So the alarm module cannot only alarm based on the deviation value of a single image, and set a threshold value for the number of images with the same degree of deviation detected. When the number of images of the same runaway degree reaches the corresponding threshold value, then the runaway alarm is made to prevent the detection system from repeatedly alarming and affecting the stability of the system.

B. System interface design

The belt deviation detection system designed in this paper uses LabVIEW software for the interface design. LabVIEW is an imaging programming language. It is able to provide users with concise, intuitive and easy-to-use programming, saving development time and easy maintenance. Segmentation and detection of belts, rollers and materials through LabVIEW calls with trained deep learning models. According to the design requirements of the belt deviation detection system. In this paper, we designed the login interface, deviation detection interface and alarm log interface. Design the program according to the functions to be implemented in each interface, in order to make the detection system more complete. The interface design of the belt deviation detection system is shown in Fig. 14.

Switch between belts via tab control at the top of the interface. In the middle is the image display window, which

is used to observe the actual status of the belt. At the bottom you can select the alarm threshold for the belt, the required belt deviation level is different for different belts, you can select "mild deviation alarm" and "heavy deviation alarm". The percentage of belt deviation can also be displayed. The direction of belt deviation and belt status are displayed on the right side of the interface by means of indicators, and the corresponding alarm can be made after selecting the corresponding deviation threshold.

The belt deviation detection system designed in this paper has been tested in the field environment and is able to complete the belt deviation detection task well under relatively complex conditions, meeting the actual needs of industrial sites and playing a key protective role for the belt conveyor.

VII. CONCLUSION

This paper proposes a deviation detection method to determine the standard position of the belt based on whether the belt is empty or not, for the situation that the camera can only monitor the edge of the belt and the rollers on one side. Distribution zones and identification of material on the belt based on the results of a multi-task learning model. By extracting pixel points from the edge of the belt and the topmost corner of the rollers, converting the coordinate system, fitting the least squares method, etc., a straight line at the edge of the belt and the connection line at the topmost corner of the rollers are fitted, and finally a belt deviation judgment model is established. Depending on the deviation value, it is classified into different ranges of deviation degree. The final result is an overall accuracy of 94.9% for the system. After the actual test results in the field, the belt deviation detection system proposed in this paper can well meet the field requirements. It can be proved that the belt deviation detection method proposed in this paper can still maintain a high accuracy rate in the face of complex working conditions and has certain practical significance.
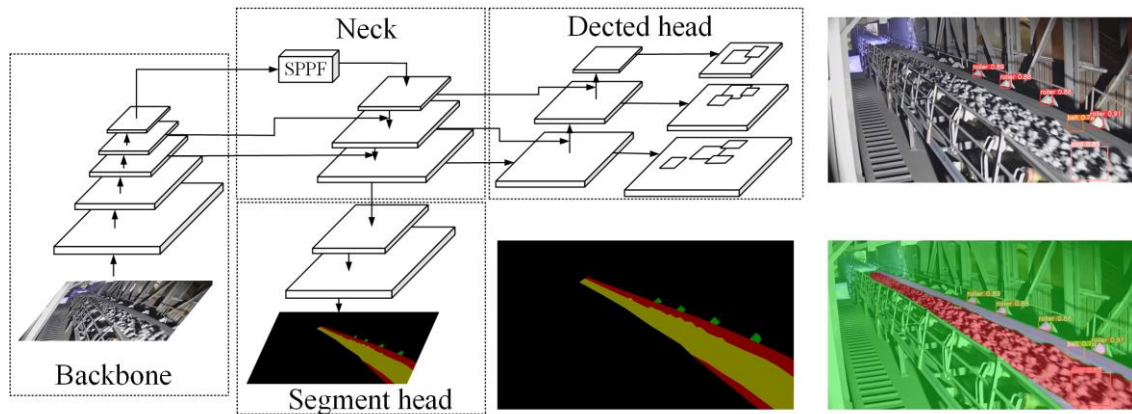
Fig. 7. Structure of multi-task learning network model

TABLE IV
TEST RESULTS OF BELT DEVIATION DETECTION METHOD FOR SINGLE-SIDE ROLLER WORKING CONDITION

Belt Status	Total number of samples	The number of judgments made	Determine the correct number	Number of misjudgments	Number of missed judgments
Normal state	987	987	987	0	0
Mild deviation	1035	1027	1027	8	0
Heavy deviation	834	834	834	0	0
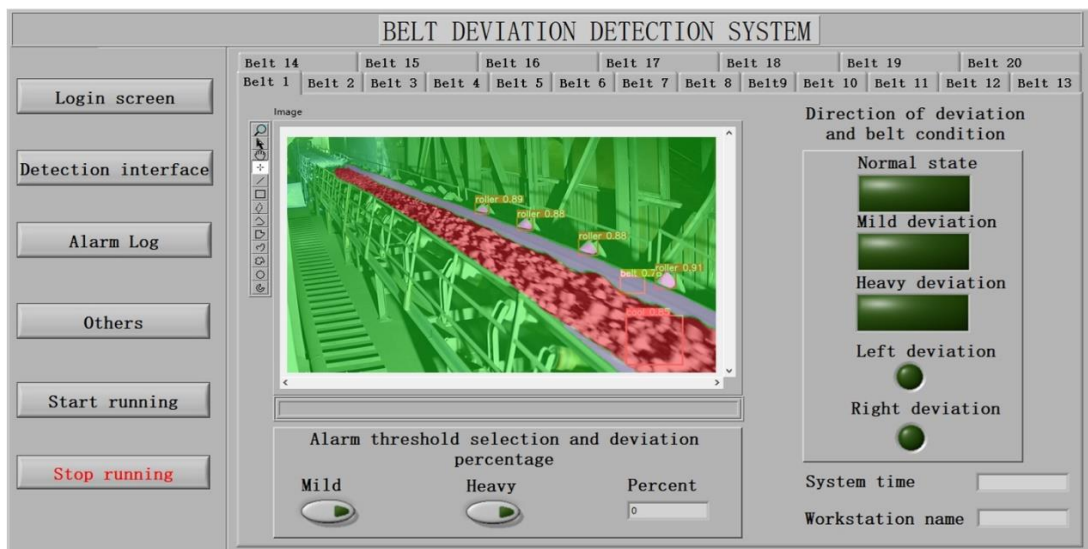
Fig. 14. System interface design

REFERENCES

[1] H. W. Ma, H. W. Fan, Q. H. Mao, X. H. Zhang, X. Wang, "Noise reduction of steel cord conveyor belt defect electromagnetic signal by combined use of improved wavelet and EMD," *Algorithms*, vol. 9, no. 4, pp. 62, 2016.

[2] Q. Y. Chu, G. Y. Meng, X. Fan, "Analysis of speed and belt deviation of the conveyor belt," *Advanced Materials Research*, vol. 1453, no. 339, pp. 444-447, 2011.

[3] W. Wang, S. Xu, Y. Teng, "Design of belt sprinkler monitoring system based on image processing technology," IAENG Internaitonal Journal of Computer Science, vol. 49, no. 1, pp. 94-100, 2022.

[4] M. Wang, K. J. Shen, C. W. Tai, Q. F. Zhang, Z. W. Yang, C. B. Guo, "Research on fault diagnosis system for belt conveyor based on internet of things and the LightGBM model," *PloS one*, vol. 18, no.3, pp. e0277352-e0277352, 2023.

[5] M. C. Zhang, K. Jiang, Y. S. Cao, M. X. Li, N. Hao, Y. Zhang, "A deep learning-based method for deviation status detection in intelligent conveyor belt system," *Journal of Cleaner Production*, vol. 363, 2022.

[6] C. Yu, Y. L. Liu, Q. H. Yang, "Research on taper detection method of roller for belt conveyor," *Journal of Physics: Conference Series*, vol. 1549, no. 4, pp. 042141, 2020.

[7] C. Zeng, J. Zheng, J. Li, "Real-time conveyor belt deviation detection algorithm based on multi-scale feature fusion network," *Algorithms*, vol. 12, no. 10, pp. 205-205, 2019.

[8] Z. F. Hu, X. Yang, Y. J. Li, Z. H. Long, A. W. Liu, X. F. Dai, X. M. Lei et al., "Research on identification technology of field pests with protective color characteristics," *Applied Sciences*, vol. 12, no. 8, pp. 3810-3810, 2022.

[9] X. M. Ma, J. M. Yang, H. Sun, Z. Y. Hu, L. X. Wei, "Feature information prediction algorithm for dynamic multi-objective optimization problems," *European Journal of Operational Research*, vol. 295, no. 3, pp. 965-981, 2021.

[10] D. Wu, M. W. Liao, W. T. Zhang, X. G. Wang, X. Bai, W. Q. Cheng et al., "YOLOP: You only look once for panoptic driving perception," *Machine Intelligence Research*, vol. 19, no. 6, pp. 550-562, 2022.

[11] L. Li, Z. F. Wang, T. Zhang, "GBH-YOLOv5: Ghost convolution with BottleneckCSP and tiny target prediction head incorporating YOLOv5 for PV panel defect detection," *Electronics*, vol. 12, no. 3, pp 561-561, 2023.

[12] O. L. Ryan, "Robustness reasoning in climate model comparisons," *Studies in History and Philosophy of Science*, vol. 85, pp. 34-43, 2021.

[13] J. Dang, X. F. Tang, S. Li, "HA-FPN: Hierarchical attention feature pyramid network for object detection," *Sensors (Basel, Switzerland)*, vol. 23, no. 9, 2023.

[14] S. Liu, Q. Lu, H. F. Qin, J. P. Shi, J. Y. Jia, "Path aggregation network for instance segmentation," *CoRR*, 2018.

[15] C. X. Dong, S. H. Xu, D. W. Dai, Y. Z. Zhang, C. Y. Zhang, Z. F. Li, "A novel multi-attention, multi-scale 3D deep network for coronary artery segmentation," *Medical Image Analysis*, vol. 85, pp. 102745-102745, 2023.

[16] H. S. Zhao, J. P. Shi, X. J. Qi, X. G. Wang, J. Y. Jia, "Pyramid scene parsing network," *CoRR*, 2016.

[17] A. Neah, M. V. Ruth, C. Nicola, T. Suzanne, "Staff knowledge, attitudes and confidence levels for fall preventions in older person long-term care facilities: a cross-sectional study," *BMC Geriatrics*, vol. 23, no. 1, pp. 595, 2023.

[18] P Zhang, S Xu, W Wang, "Belt Deviation Detection System Based on Deep Learning under Complex Working Conditions," IAENG International Journal of Applied Mathematics, vol. 53, no. 3, pp. 863-868, 2023.

PENG ZHANG was born in Inner Mongolia Autonomous Region, P. R. China, received the B.S. degree in Measurement and Control Technology and Instruments from University of Science and Technology Liaoning, Anshan, P. R. China, in 2021.

He is currently pursuing the M.S. degree in Control Science and Engineering with University of Science and Technology Liaoning, Anshan, P. R. China. His research interest is machine vision.

SHAOCHUAN XU was born in Liaoning Province, P. R. China, received the B.S. degree in automation from University of Science and Technology Liaoning, Anshan, P. R. China, received the M.S. degree in control science and engineering from University of Science and Technology Liaoning, Anshan, P. R. China, in1995, and 2004.

He is currently a professor in the School of Control Science and Engineering, University of Science and Technology Liaoning, Anshan, P. R. China. He published more than 20 academic papers, more than 20 patents and software copyrights. His research interests include research on industrial intelligent control and machine vision.

MINGHAO MA was born in Liaoning Province, P. R. China, received the B.S. degree in Communication Engineering from University of Science and Technology Liaoning, Anshan, P. R. China, in 2022.

He is currently pursuing the M.S. degree in Electronic Information with University of Science and Technology Liaoning, Anshan, P. R. China. His research interest is machine vision